REVIEW: THE MICROHARDNESS OF NON-CRYSTALLINE MATERIALS

F. J. BALTÁ CALLEJA
Instituto de Estructura de la Materia, CSIC, Serrano 119, 28006 Madrid, SPAIN.
E-mail : iemd300@csic.es

D.S. SANDITOV
Buryat State University, Smolina 24a, 670000 Ulan-Ude, RUSSIA, E-mail : sanditov@bsu.ru

V.P. PRIVALKO
Institute of Macromolecular Chemistry, National Academy of Sciences of Ukraine, Kharkiv Chaussee 48, 02160 Kyiv, UKRAINE, E-mail : privalko@iptelecom.net.ua

Abstract

Hardness is defined as a phenomenological measure of resistance of a material to shear stresses under local volume compression. It is shown that this definition may serve as a theoretical basis for existing empirical relationships between the Vickers microhardness H_V and the various phenomenological, packing density-sensitive parameters of non-crystalline materials, including among them, the internal pressure, the glass transition temperature T_g, the excess enthalpy, and the free volume fraction at T_g.

Key words: Disordered materials; mechanical properties of materials; deformation and plasticity; hardness; yield; elastic parameters; enthalpy.

1. Introduction

Hardness H is an important mechanical property that may be defined as a measure of the resistance of a material to the application of a contact load. A common definition to measure the H is the relationship between the peak contact load P and the projected area of impression A [1-3]. This impression, A, is often, of the order of 10-100 squared microns. Hence, the experimental values of H are commonly referred to as "microhardness". It is obvious that a single value of H would be sufficient to characterize the microhardness of any polycrystalline material, in so far as A, by far exceeds the characteristic size of structural heterogeneities involved (microcrystallites). Nevertheless, both, size and relative content of the latter (e.g., chain-folded and chain extended lamellar crystals in semi-crystalline polymers) proved to be extremely important structural parameters controlling the experimental values of H [4-8].

In contrast, large-scale structural heterogeneities are believed to be absent in non-crystalline (glassy) materials [9,10]. However, a random distribution of densely-packed domains of quasi-crystalline order within a loosely-packed matrix has been accepted as a reasonable phenomenological schematics of the structure of glasses [11,12]. Within this context, any macroscopic property of a glassy material may be expected to depend on a phenomenological, packing density-sensitive parameter, such as internal pressure, free volume fraction or other appropriately chosen degree of residual disorder (with respect to the fully ordered, crystalline state). The aim of this review is the analysis and discussion of the correlations between H and the various phenomenological structural parameters for non-crystalline materials.

2. Microhardness and deformation micro-mechanics of indentation

2.1. Microhardness as a measure of resistance to shear stresses under volume compression

Penetration of a brittle material with a microindenter (typically, of conical or pyramidal shape with the apex angle above 120°) loaded by a force P produces a surface microimpression of area A from which the microhardness $H = P/A$ may be derived [2,8,13]. The use of a diamond pyramid with the apex angle of 136° leads to the Vickers microhardness H_V [MPa],

$$H_V = 1854\frac{P}{d^2}, \tag{2.1}$$

where the dimensions of force P and of impression diameter d are [Newton] and [millimeters], respectively.

The stresses under a Vickers pyramid and under a spherical indenter turn out to be similar. Therefore, the stress distribution under the former may be described by Hertz equations derived from treatment of the contact problem for sphere impression into a flat surface [1,2]. The complex stress state under a sphere is characterized by compression stresses along (and symmetrical to) the vertical axis, and by stretching stresses near the specimen surface. The maximum pressure at the center of contact surface (corresponding to the yield stress at the point of spherical impression) is

$$P_0 = \frac{3}{2\pi}\cdot\frac{P}{r^2}, \tag{2.2}$$

where r is the radius of pressure circle (i.e., contact surface). The normal stress component σ_z along the vertical symmetry axis z is (Fig. 1)

$$\sigma_z = -P_0\frac{r^2}{z^2 + r^2}\,.$$

It is obvious that $\sigma_z = -P_0$ at $z = 0$ (i.e., at the contact surface), while equal stresses along transversal axes x and y are

$$(\sigma_x)_z = (\sigma_y)_z = (1-\mu)P_0\left(1-\frac{z}{r}arctg\frac{z}{r}\right)+\frac{P_0}{2}\left(\frac{r^2}{z^2+r^2}\right),$$

where μ is the Poisson's coefficient. It can be easily verified that these stresses at $z = 0$ are described by a more simple expression,

$$(\sigma_x)_{z=0} = (\sigma_y)_{z=0} = -\frac{P_0}{2}(1+2\mu). \qquad (2.3)$$

The special case of $\mu = 0.5$ corresponds to equal main stress components (i.e., isotropic volume compression),

$$(\sigma_x)_{z=0} = (\sigma_y)_{z=0} = -P_0\,, \qquad (\sigma_z)_{z=0} = -P_0\,; \qquad (2.4)$$

whereas the more general case of $\mu < 0.5$ for real materials corresponds to

$$(\sigma_x)_{z=0} = (\sigma_y)_{z=0} < P_0$$

As a result, at the center of compression area the shear stress is generated,

$$\tau = \frac{\sigma_x - \sigma_z}{2}. \qquad (2.5)$$

Remarkably, the maximum of τ is reached within the bulk material at a distance of $z = 0.47\,r$ from the surface, rather than at the surface itself (Fig. 1). At this depth, the maximum shear stresses are three times higher than the maximum shear stress at the contact surface ($\tau_m = 3\,\tau_{z=0}$), i.e.,

$$\tau_m = 3\frac{(\sigma_x)_{z=0} - (\sigma_z)_{z=0}}{2}. \qquad (2.6)$$

Substitution of $(\sigma_x)_{z=0}$ and $(\sigma_z)_{z=0}$ from eqs. (2.3) and (2.4), of P_0 from eq. (2.2) and of $r = 0.35\,d$ yields, finally [1] :

$$\tau_m = 2925\frac{P}{d^2}(1-2\mu), \tag{2.7}$$

where the dimensions of P, d and τ_m are [Newton], [millimeters] and [MPa], respectively.

As can be inferred from the above analysis of the stressed state under the Vickers indenter, a local plastic shear deformation should occur in the region of isotropic compression at a distance of the order of half-contact radius below the material surface. The deeper the penetration at $P = const$, the larger is the contact area, and the lower are the shear stresses τ. The final penetration depth is reached when the maximum shear stress τ_m matches the yield stress σ_y of a material, above which the plastic deformation sets on, i.e.,

$$\tau_m \cong \sigma_y . \tag{2.8}$$

Within this context, a more appropriate definition of the microhardness would probably be a measure of the resistance to shear deformations under conditions of isotropic compression, as implied by eq. (2.7), rather than an average normal pressure H_V as defined by eq. (2.1). For practical reasons, however, the latter equation is usually preferred, in so far, as it does not contain an additional material parameter (Poisson's coefficient μ). Nevertheless, in the following discussion concerning the physical significance of microhardness the basic eq. (2.7) will be invoked.

By elimination of the ratio P/d^2 from eqs. (2.1) and (2.7), one obtains

$$H_V = \frac{0{,}6338}{(1-2\mu)}\tau_m . \tag{2.9}$$

The latter eq. (2.9) may be used to estimate, say, τ_m from known values of H_V and μ, and vice-versa.

It is obvious that H_V should correlate with τ_m for materials with similar values of μ. This is the case of inorganic optical glasses with $\mu = 0.22$-0.26 (Table 1.1), for which

$$H_V/\tau_m \cong 1 . \qquad (2.10)$$

In contrast, for linear amorphous polymers with $\mu = 0.33$-0.38 (Table 1.2) this ratio becomes twice as high, i.e.,

$$H_V/\tau_m \cong 2. \qquad (2.11)$$

Thus, these two latter equations may be regarded as an empirical evidence supporting our earlier claim that microhardness is basically a measure of resistance to shear deformations under conditions of isotropic compression. From eq. (2.9), a constancy of the ratio H_V/σ_y is also implied for materials with similar values of Poisson's coefficient μ. This is consistent with the following empirical relationship for glassy polymers [14]:

$$H_V/\sigma_y \cong const \cong 1.9 \qquad (2.12)$$

A justification of this empirical relationship is given in the next section.

2.2. Microhardness and yield stress

In metals, the general relationship between the Vickers hardness H_V and the yield point σ_y is expressed as [2,15],

$$H_V/\sigma_y \cong 3 . \qquad (2.13)$$

This relationship was derived theoretically as a solution of the contact problem for a rigid-plastic body, and proved experimentally for metals with high Young's modulus E and low

yield stress σ_y (i.e., those with $\sigma_y/E \leq 0.001$). Such approach is, however, inapplicable for non-crystalline materials like organic polymers and inorganic glasses which are characterized by $0.05 < \sigma_y/E < 0.1$. In this case, the solution of the elastic-plastic problem for expansion of a spherical cavity within a solid [15] appears more appropriate. It is argued [16] that the material under an indenter should be forced either inwards along the radial directions (in the spherical cavity regime), or outwards in the direction of a free surface (in the rigid piston regime), respectively. In the latter case, the forced-out material is expected to form bulges around the impression.

Typical profiles for the Vickers impression cross-sections at room temperature for aluminum (1), poly(methyl methacrylate) (2) and window silicate glass (3) are shown in Fig. 2 [17]. As could be expected from considerations of the sliding field lines under a flat rigid piston, the impression on the Al is, in fact, surrounded by bulges. In contrast, "buried" impressions without measurable bulges predicted for a spherical deformation regime under an indenter [16], are observed for, both, organic and inorganic glasses.

As follows from the solution of the problem of the spherical cavity, nucleation and expansion in an infinite continuum [15], the ratio of the relevant stress H to the yield point σ_y is given by

$$\frac{H}{\sigma_y} = \frac{2}{3}\left[1 + \ln\frac{E}{3(1-2\mu)\sigma_y}\right]. \qquad (2.14)$$

It turns out that the inequality, $H_V/\sigma_y < H/\sigma_y$, is a typical case for polymer glasses, although sometimes the values of this ratio may be of comparable magnitude [16]. It seems obvious that the stresses required to support the material in bulges around the impression (which

can be represented as a semi-spherical cavity), are lower than those developed under the spherical cavity case. Hence, $H_V < H$ should be expected.

It can be argued that eq. (2.14) may be also applicable for non-crystalline materials, provided the factor 2/3 on the r.h.s. is replaced by an empirical parameter $c < 2/3$, i.e.

$$\frac{H_v}{\sigma_y} = c\left[1 + \ln\frac{E}{3(1-2\mu)\sigma_y}\right]. \qquad (2.15)$$

The available experimental data for organic and inorganic glasses may be reasonably fitted into this latter empirical equation assuming $c \cong 0.5$ [17]. Eq. (2.15) can then be rewritten as

$$\frac{H_v}{E} \cong 0{,}5\left[1 - \ln 3(1-2\mu)\frac{\sigma_y}{E}\right]\cdot\frac{\sigma_y}{E} \quad . \qquad (2.16)$$

Thus, the ratio σ_y/E (hence, the yield point σ_y) may be estimated [16,17] by fits to the theoretical H_V/E vs. σ_y/E plots for non-crystalline materials with known values of H_V, E and μ (see Fig. 3).

As can be seen from Table 1.3 [17], the values of σ_y for poly(methyl methacrylate) calculated by eq. (2.16) from experimental data for Young's modulus E and microhardness H_V assuming $\mu = 0.33$, are reasonably close to the available measured values [16,18,19].

The empirical factor $c = 0.5$ in eq. (2.16) is, in fact, an approximation of $c \cong 0.47$ which can be derived from eq. (2.15) by substitution of typical experimental averages, $\sigma_y/E \cong 0.05$, $H_V/\sigma_y \cong 1.9$ and $\mu \cong 0.33$ [14,16,20]. The σ_y/E and μ values for different polymers are of

the same order of magnitude (moreover, they enter eq. (2.16) under the logarithm), whereas the linear correlation between H_V and σ_y as expressed by eq. (2.12), is the result of treatment of relevant experimental data for a large number of polymers [14]. Thus, eq. (2.16) with the statistically reliable value $c = 0.5$ may be recommended for estimation of the yield stress σ_y for glassy polymers. It is, additionally, noteworthy that substitution of typical average values, $\sigma_y/E \cong 0.002$ and $\mu \cong 0.25$, for carbon steels into eq. (2.16) yields $H_V/\sigma_y \cong 2.9$ which is virtually identical to eq. (2.13) for metals.

3. Microhardness and structure of disordered materials

3.1. Internal pressure

As argued in the foregoing, formation of an impression under the micro-indenter is the result of an irreversible (plastic) deformation which sets on beyond the yield point σ_y. Thus, σ_y should exceed (or, at least, be equal to) the energy of interparticle interactions, one measure of which is the internal pressure P_i [21,22]. In fact, the maximum internal pressure P_m (corresponding to the maximum of interparticle interactions energy) may be interpreted as the yield stress σ_y of a material [23]. Thus, one should expect the correlation, $H_V \sim \sigma_y \sim P_m$.

According to the standard definition [21,22], the internal pressure P_i is the isothermal derivative of internal energy U over volume V,

$$P_i = \left(\frac{\partial U}{\partial V}\right)_T . \qquad (3.1)$$

expansive) strains [21,22]. Under quasi-static, uniaxial extension the elastic stress P_i is numerically equal to the applied external mechanical stress which is proportional, by definition, to the relative extension (Hooke's law) , $\Delta l/l_0 = \Delta r/r_0$. Hence,

$$P_i = E\frac{\Delta r}{r_0}, \qquad (3.2)$$

where E is the Young's modulus, $\Delta r/r_0$ is the relative extension of an interparticle bond, and r_0 is the mean (equilibrium) interparticle distance.

Let us consider the expansion of the potential energy of binary interparticle interactions $u(r)$ into a Taylor series of displacements, $x = \Delta r = r - r_0$, of a particle with respect to its equilibrium position (Fig. 4). Truncation of the series after the fourth term yields

$$u \cong u_0 + \left(\frac{du}{dr}\right)_{r_0} \cdot x + \frac{1}{2}\left(\frac{d^2u}{dr^2}\right)_{r_0} \cdot x^2 + \frac{1}{6}\left(\frac{d^3u}{dr^3}\right)_{r_0} \cdot x^3 . \qquad (3.3)$$

Taking into account that $(du/dr)_{r=r_0} = 0$ at the minimum of the function $u(r)$ (Fig. 2.1), and making the substitutions

$$a = \left(\frac{d^2u}{dr^2}\right)_{r=r_o} , \quad b = -\left(\frac{d^3u}{dr^3}\right)_{r=r_o} , \qquad (3.4)$$

(where a and b are defined as harmonic and an-harmonic factors in the above series), one derives from eq. (3.3) :

$$u \cong u_0 + \frac{ax^2}{2} - \frac{bx^3}{6} . \qquad (3.5)$$

The latter equation may be used to define the force of interparticle interactions, $f = -(du/dx)$, as

$$f \cong -ax + \frac{b}{2}x^2 . \qquad (3.6)$$

As can be seen from Fig. 4, the force $f = -(du/dr)$ passes through maximum at the inflexion point of function $u(r)$. Therefore, the critical extension $x_m = (r_m - r_0)$ of an interparticle bond corresponding to a maximum force f_m, may be derived from eq. (3.6) using the standard condition, $\left(df/dx\right)_{x=x_m} = 0$, i.e., $x_m = \Delta r_m = a/b$. Thus, the relative critical strain of an interparticle bond is given by:

$$\frac{\Delta r_m}{r_0} = \frac{a}{br_0} . \qquad (3.7)$$

The physical implication of eq. (3.7) is straightforward. At a given particle displacement exceeding the critical value $x_m = \Delta r_m$ the lattice anharmonicity begins to manifest itself through the relevant anharmonicity factor b. As a result, non-linearity of the interparticle force $f(x)$ sets on.

In view of these considerations, a correlation between the ratio $\Delta r_m/r_0$ at the l.h.s. of eq. (3.7) and the classical measure of anharmonicity of lattice vibrations, (Grüneisen parameter γ) should be expected. The classical Grüneisen equation for the cubic coefficient of thermal expansion [21,24],

$$\alpha = \gamma \frac{C_v}{KV}\,, \tag{3.8}$$

can be compared with a similar Frenkel equation [25]

$$\alpha = \frac{bk_B}{2ar_0^2 K}\,, \tag{3.9}$$

where $C_V \cong 3\ k_B$ is the isochoric heat capacity, $V \cong r_0^{\,3}$ is the volume, K is the bulk modulus, and k_B is the Boltzmann's constant. Multiplying the latter eq. (3.9) by $3r_0/3r_0$, one obtains

$$\alpha = \left(\frac{br_0}{6a}\right)\left(\frac{C_v}{KV}\right), \tag{3.9a}$$

which is identical to eq. (3.8), provided [26]

$$\gamma = \frac{br_0}{6a}. \tag{3.10}$$

Eq. (3.10) can be also derived by means of more rigorous procedures [21,27]. In this formulation, the critical strain defined by eq. (3.7) turns out to be proportional to the reciprocal Grüneisen parameter [23],

$$\frac{\Delta r_m}{r_0} = \frac{1}{6\gamma}. \tag{3.11}$$

Let us assume that Hooke's law (3.2) applies, in first approximation, up to the limiting bonding strain (3.11). Then, by substituting the latter equation into the former, one derives [21,28]:

$$P_m = \left(\frac{1}{6\gamma}\right)E. \qquad (3.12)$$

In this representation, the maximum internal pressure of an equilibrium material P_m (and, by implication, its microhardness H_V) should be higher, the stronger are the relevant inter-particle interactions (i.e., the higher the Young's modulus E and/or the lower the Grüneisen parameter γ).

3.2. Elastic parameters

It has been tacitly assumed that the validity of eq. (3.12) is limited to equilibrium solids, whereas the non-crystalline material (glassy) represents a non-equilibrium state [12,29,30]. As can be inferred from the schematic diagram in Fig. 5, a glassy material is structurally similar to an equilibrium liquid by its excess (with respect to the equilibrium crystal state), "configurational" properties (such as excess volume, excess enthalpy and/or excess entropy). However, by its internal mobility the glassy material is similar to an equilibrium crystal. In terms of continuum mechanics, an equilibrium (crystalline) material has no stresses in its reference state [31], whereas the reference states of an amorphous material are metastable, quasi-equilibrium states which are, however, internally stressed [32]. On a macroscale (i.e., at distances above the relevant correlation length ξ), the internal stresses within a glass are assumed to have a zero average, whereas on a length scale below ξ, one should distinguish between stabilizing (negative) stresses in the isolated domains of a soft, unbuckled material, and destabilizing (positive) stresses in a rigid continuous matrix which has undergone structural buckling [32].

The immediate practical implication is that the weak (soft) vibration modes of a soft, unbuckled material within isolated domains of size ξ are those making a dominant contribution

to the Grüneisen constant in eq. (3.12). In this case, the parameter γ in eq. (3.12) should be understood as the so called "lattice Grüneisen constant γ_L" [33,34] which is a measure of vibration anharmonicity of relatively weak interactions (e.g., interchain forces in polymers, and forces between ions of earth metals and off-bridge oxygen atoms of ionic sublattices in silicate glasses). To avoid confusion with the "thermodynamic Grüneisen constant γ_T ", it would be desirable to express the constant γ in eq. (3.12) through other, more easily measurable material parameters.

Multiplying the basic eq. (3.8) by Gk_BT/Gk_BT and assuming $C_V \cong 3\ k_B$, one obtains [35] :

$$\gamma = (K/3G)\ [\alpha T\ (GV/k_BT)]\ , \qquad (3.13)$$

where G is the shear modulus. In principle, eq. (3.13) should also apply for an equilibrium liquid, provided G is the instantaneous (i.e., solid-like) shear modulus. In this case, the product GV is essentially the activation energy for viscous flow E_η , which is related to the free volume fraction f as $E_\eta/k_BT \cong 1/f$, while $\alpha T \cong f\ ln\ (1/f)$ [28]. We assume that the same equations remain valid for a glassy material, the only difference being that the free volume fraction f is no longer a function of temperature but is frozen-in at the glass transition temperature T_g. In other words, f_g remains constant in the glassy state below T_g . According to these considerations, and using the standard formula of elasticity theory,

$$\frac{K}{G} = \frac{2}{3}\left(\frac{1+\mu}{1-2\mu}\right)$$

the eq. (3.13) can be rewritten as [23]:

$$\gamma = \frac{2\ln(1/f_g)}{9}\left(\frac{1+\mu}{1-2\mu}\right) \quad . \tag{3.14}$$

Thus, the factor $1/A = \dfrac{9}{2\ln(1/f_g)}$ may be regarded as a phenomenological measure of the contribution of residual disorder to the vibration anharmonicity of a non-crystalline material.

Substitution of eq. (3.14) into (3.12) yields

$$P_m = A\left(\frac{1-2\mu}{1+\mu}\right)E/6. \tag{3.15}$$

In view of fairly narrow limits of variation of the fixed free volume fraction f_g ($\cong$ 0.015-0.030), for practical purposes the factor A ($\cong$ 0.78-0.93) may be approximated as unity, i.e.,

$$P_m \cong \frac{1-2\mu}{6(1+\mu)}E. \tag{3.16}$$

Thus, the maximum internal pressure P_m (microhardness H_V) of a non-crystalline material becomes a function of its main elastic parameters which are readily obtained by experiment.

As can be easily verified (Tables 2.1-2.3), the available experimental data for many inorganic glasses [28,36-39] are in reasonable agreement with eq. (3.16). Moreover, these data are also consistent with the basic assumption, $P_m/H_V \cong 1$. The notable exceptions are the boron anhydride, B_2O_3 (Table 2.3), and sodium-borate glasses containing 5-20 mol % of Na_2O. It can be argued that in the latter case the concentration of $[BO_4]^-$ anions changes due to the transformation of a fraction of boron atoms from triple to quarternary coordination by oxygen [40]. The negative charges of $[BO_4]^-$ anions are compensated by positively charged Na^+ cations

within the $[BO_4]^-$ Na^+ complex, the higher the Na_2O contents. As a result, the ratio P_m/H_V increases and levels-off around unity at Na_2O contents above 20 mol. %.

3.3. Excess enthalpy

According to current concepts [41], the inelastic (irreversible) deformation of a non-crystalline material above the yield point σ_y starts by the breakdown of a rigid glassy quasi lattice and is followed up by liquid-like, co-operative rearrangements of relevant structural units ("plastic flow" phenomenon). As a typical example, after plastic deformation the Poisson's coefficient for polycarbonate increases from a solid-like value of 0.35 to a liquid-like value of 0.42 [42]. In this context, a small volume element of a glassy material under the indenter is assumed to be "forced" by a plastic flow mechanism into the state of a hypothetical melt at $T' << T_g$. As illustrated in Fig. 5, this is equivalent to an exothermal transition from the high-energy glassy state (H_{glass}) into the low-energy melt state (H_{melt}). The heat liberated during this transition, $\Delta H = H_{melt} - H_{glass}$, can be envisioned as a new measure of the strength of a glassy quasi lattice, alternative to the σ_y [43].

Thus, assuming $\sigma_y \sim \Delta H$, one derives from eq. (2.12)

$$H_V \cong C'\Delta H \cong C'<\Delta c_p>(T' - T_g), \qquad (3.17)$$

where C' is a numerical parameter, and $<\Delta c_p> = c_{p,\,melt} - c_{p,\,glass}$ is the mean difference between the specific heat capacities of a substance in the melt and in the glassy state, respectively, in the temperature interval between the temperature of measurement T' and the glass transition temperature T_g [44,45].

The linear increase of H_V with T_g, as predicted in eq. (3.17) by the condition, $C'<\Delta c_p> \cong const$, is consistent with the available experimental data for silicate glasses (Fig.

6) and for several series of glassy polymers (Fig. 7) [43,46]. The apparent constancy of the product $C'<\Delta c_p>$ implies either the constancy of each of both terms, or the inverse proportionality between them. However, the observed scatter of experimental data on the typical H_V vs. T_g plot (Fig. 7) suggests that, at least, one of the above assumptions may not be strictly valid.

In principle, an additional source of the scattering of data may be the dependence of T_g on the mechanical and/or thermal history of a studied sample. As can be inferred from the schematic diagram in Fig. 5, the T_g value (hence, the excess enthalpy ΔH at T') for a given sample will be higher ($T_g'' > T_g'$), the higher the cooling rate of an equilibrium melt at the same pressure, or the higher the densification pressure at the same cooling rate. This effect, however, proves to be of minor importance [43].

3.4. Free volume fraction

As argued above, a glass may be defined as an expanded (with respect to an equilibrium crystal), internally stressed material with a liquid-like structural disorder frozen-in at T_g (Fig. 5). One of the experimental manifestations of the arrest of external (configurational) degrees of freedom on cooling an equilibrium liquid through and below T_g, is a sudden drop of the maximum internal pressure [47]. Therefore, the internal pressure P_m' of a non-equilibrium, metastable glass at T' << T_g becomes significantly smaller than that (P_m) for a hypothetical equilibrium melt (Fig. 8).

In the free volume (hole) formulation [48], for an equilibrium liquid the hole formation probability will be the hole fraction,

$$f = N_h/N \cong exp\ (-X)\ , \qquad (3.18)$$

while the maximum internal pressure P_m is simply the ratio of hole energy to the hole volume,

$$P_m = \frac{\varepsilon_h}{v_h}. \qquad (3.19)$$

(here N_h is the number of holes, N is the total number of lattice sites, $X = (\varepsilon_h + v_h P)/k_B T$, ε_h and v_h are the hole formation energy and hole volume, respectively). The internal pressure of a liquid at T_g may be calculated by eq. (3.19) with the hole energy in the numerator derived from eq. (3.18) as

$$\varepsilon_h = k_B T_g \, ln \, (1/f_g), \qquad (3.20)$$

while the deficit of the internal pressure of a glass, P_m', may be accounted for as [49]

$$P_m' = P_m (1 - A). \qquad (3.21)$$

Assuming $\sigma_y \cong P_m'$, one may write, finally [49]

$$\sigma_y = \left(\frac{C_2 k_B}{v_h} \right) T_g, \qquad (3.22)$$

where

$$C_2 = \ln\left(\frac{1}{f_g}\right)\left[1 - \frac{2}{9}\ln\left(\frac{1}{f_g}\right)\right] \cong const \approx 0{,}66.$$

The linear dependence of σ_y on T_g predicted by eq. (3.22) for substances with similar values of v_h is, in fact, consistent with the available experimental data for organic polymers (Fig. 9). From the plots of Figs. 6 and 7, this result may be regarded as an additional evidence for the assumed proportionality between H_V and σ_y (see above).

Acknowledgements

This work was supported in part by the project INTAS-97-1936. Grateful acknowledgement is also due to MCYT, Spain (Grant BFM2000-1474), for the generous support of this investigation.

References

[1] Shreiner, L.A., "The Hardness of Brittle Solids". (OGIZ, Leningrad-Moscow, 1949) (in Russian)

[2] Tabor, D., "The Hardness of Metals". (Oxford C. Press, New York, 1951).

[3] Gogoberidze, D.B., "The Hardness and Techniques for its Measurement". (Mashgiz, Moscow, 1952) (in Russian).

[4] Baltá Calleja, F.J., *Trends Polym. Sci.* **2** (1994) 419.

[5] Baltá Calleja, F.J., Giri, L., Ward, I.M., Cansfield, D.L.M., *J. Mater. Sci.* **30** (1995) 1139

[6] Flores, A., Baltá Calleja, F.J., Bassett, D.C., *J. Polymer Sci. Phys.* **37** (1999) 3151

[7] Baltá Calleja, F.J., Flores, A., Ania, F., Bassett, D.C., *J. Mater. Sci.* **35** (2000) 1315.

[8] Baltá Calleja, F.J., Fakirov S. "Microhardness of Polymers", (Cambridge University Press, Cambridge, 2000).

[9] Hosemann, R., Bagchi, S.N., "Direct Analysis of Diffraction by Matter". (North Holland, Amsterdam, 1962).

[10] Uhlmann, D.R., *Faraday Disc. Chem. Soc.* **68** (1979) 87.

[11] Haward, R.N., (ed.), "The Physics of Glassy Polymers". (Applied Science Publ. Ltd., London, 1973)

[12] Zallen, R., "The Physics of Amorphous Solids". (John Wiley & Sons, New York, 1983).

[13] O'NeilL, H., "Hardness Measurement of Metals and Alloys". (Chapman & Hall, London, 1967).

[14] Sinani, A.B., Stepanov, V.A., Hardness and limiting high elasticity of amorphous polymers. In: "Hardness Research", (USSR Institute of Metrology. Izd. Standartov, Moscow, p. 180, 1967) (in Russian).

[15] Hill, R., "Mathematical Theory of Plasticity". (Clarendon Press, London, 1950).

[16] Ainbinder, S.B., Laka, M.G., *Mekh. Polim.* **No 1** (1968) 90.

[17] Sanditov, D.S., *Izv. VUZ'ov : Fizika* **No. 10** (1969) 111.

[18] Lazurkin, Yu.S., Fogelson, R.L., *Zhurn. Tekh. Fiz.* **21** (1954) 267.

[19] Regel, V.R., Berezhkova, G.V., The limit of forced elasticity of amorphous polymers under uniaxial compression. In: "Selected Problems of the Strength of Solids". (Izdat. Akad. Nauk USSR, Moscow, p. 375, 1959) (in Russian).

[20] Kuritsyna, A.D., Meinster P.G., *Zav. Lab.* **28** (1962) 491.

[21] Burshtein, A.I., "Molecular Physics". (Nauka, Novosibirsk, 1986) (in Russian).

[22] Croxton, C.A., "Liquid State Physics". (Cambridge University Press, Cambridge, 1974).

[23] Kozlov, G.V., Sanditov, D.S., "Anharmonic Effects and Physical-Mechanical Properties of Polymers". (Nauka, Novosibirsk, 1994) (in Russian).

[24] Kittel, C., "Introduction to Solid State Physics". (John Wiley & Sons, New York, 1956).

[25] Frenkel, J., "Introduction to the Theory of Metals". (OGIZ, Leningrad, 1948) (in Russian).

[26] Sanditov, D.S., Mantatov, V.V., *Fiz. Khim Stekla* **9** (1983) 287.

[27] Leibfried, G., "Microscopic Theory of Mechanical and Thermal Properties of Crystals". (John Wiley & Sons, New York, 1956).

[28] Sanditov, D.S., Bartenev, G.M., "Physical Properties of Disordered Structures". (Nauka, Novosibirsk, 1982) (in Russian).

[29] Kobeko, P.P., "Amorphous Substances". (USSR Acad. Sci. Publ., Leningrad, 1952) (in Russian).

[30] MacKenzie, J.D. (Ed.), "Modern Aspects of the Vitreous State" (3 Volumes.) (Butterworths, London, 1960-1964).

[31] Born, M., Huang, H., "Dynamical Theory of Crystal Lattices". (Oxford University Press, Oxford, 1954).

[32] Alexander, S., *Phys. Rep.* **296** (1998) 65.

[33] Wada, Y., Itani, A., Nishi, T., Nagai, S., *J. Polymer Sci.* **A2-7** (1969) 201.

[34] Warfield, R.W., *Makromol. Chem.* **175** (1974) 3285.

[35] Sanditov, D.S., Mantatov, V.V., *Fiz. Khim Stekla* **17** (1991) 174.

[36] Bokin, P.Ya., *Optiko-Mekh. Prom.* **No 11** (1963) 27.

[37] Mazurin, O.V., Streltsyna, M.V., Shvaiko-Shvaikovskaya, T.P., "Properties of Glasses and Glass-Forming Melts" (6 Volumes) (Nauka, Moscow, 1973-1997) (in Russian).

[38] Sanditov, D.S., Mamoshin, V.L., Arkhipov, V.G., *Fiz. Khim. Stekla* **19** (1993) 593.

[39] Sanditov. D.S., Sangadiev, S.Sh., *Fiz. Khim. Stekla* **24** (1998) 741.

[40] Nemilov, S.V., *Fiz. Khim. Stekla* **23** (1997) 3.

[41] Stachurski, Z.H., *Prog. Polym. Sci.* **22** (1997) 407.

[42] Skolnik, J., Perchak, D., Yaris, R., Schaefer, J., *Macromolecules*, **17** (1984) 2332.

[43] Baltá Calleja, F.J., Privalko, E.G., Fainleib, A.M., Shantalii, T.A., Privalko, V.P., *J. Macromol. Sci.- Phys.* **B39** (2000) 131.

[44] Privalko, V.P., "Molecular Structure and Properties of Polymers". (Khimia, Leningrad, 1986) (in Russian).

[45] Privalko, V.P., Novikov, V.V., "The Science of Heterogeneous Polymers : Structure and Thermophysical Properties". (Wiley, Chichester, 1995).

[46] Baltá Calleja, F.J., Privalko, E.G., Sukhorukov, D.I., Fainleib, A.M., Sergeeva, L.M., Shantalii, T.A., Shtompel, V.I., Monleon Pradas, M., Gallego Ferrer, G., Privalko, V.P., *Polymer* **41** (2000) 4699.

[47] Bagley, E.B., Scigliano, J.M., *Polymer Eng. & Sci.* **11** (1971) 320.

[48] Smith, R.P., *J. Polymer Sci.* **A-2**(8) (1970) 1337.

[49] Sanditov. D.S., Sangadiev, S.Sh., *J. Polymer Sci.* **A 41** (1999) 977.

Table 1.1

Mechanical properties of inorganic optical glasses (Bokin, 1963 ; Sanditov, 1969)

Glass	E / kg mm^{-2}	μ	H_V / kg mm^{-2}	τ_m / kg mm^{-2}	H_v / τ_m	H_v / E
K8	7920	0,225	579	503	1,1	0,073
BK10	7516	0,250	553	435	1,3	0,075
BPh12	6107	0,262	461	347	1,3	0,075
TPh3	5469	0,219	424	326	1,1	0,075
Ph2	5473	0,220	412	365	1,1	0,073
Ph4	5466	0,223	412	361	1,1	0,075
TPh1	5355	0,225	392	341	1,1	0,077

Table 1.2

Mechanical properties of linear amorphous polymers

Polymer	E / GPa	μ	H_V / τ_m	P_m / MPa	W_{coh} / MPa
Polycarbonate	3,7	0,35	2,1	376	384
Poly(methyl methacrylate)	4,0	0,33	1,9	344	348
Polystyrene	4,1	0,37	2,4	389	334
Poly(vinyl chloride)	4,3	0,38	2,6	374	389

Table 1.3

Microhardness and yield stress of poly(methyl methacrylate)

T / ° C	H_V	E	σ_y	σ_y*	H_V / σ_y
	kg mm^{-2} **				
25	18,6	375	10,5	11,2	1,8
40	13,2	340	6,8	8,5	1,9
50	11,0	263	5,1	–	2,1
60	9,0	253	3,9	7,0	2,3
80	6,0	172	2,7	5,0	2,2

* experimental values from uniaxial compression tests (Regel, Berezhkova, 1959)

** 1 kg/mm^2 = 9.81 MPa

Table 2.1

Mechanical properties of silicate glasses (Sanditov, Sangadiev, 1998)

Glass	μ	E / kg mm^{-2}	H_V / kg mm^{-2}	P_m / kg mm^{-2}	P_m / H_v
SiO_2	0,017	7450	693	700	1,01
K_2O-SiO_2 :					
K_2O, mol. %					
12,1	0,230	5412	406	396	0,98
15,8	0,225	5323	374	398	1,06
19,6	0,250	4848	364	330	0,91
26,4	0,270	4821	337	291	0,86
K 8	0,225	7920	579	593	1,02
TK 6	0,277	7913	600	461	0,77
BK 6	0,212	7640	500	605	1,21
BK 10	0,250	7516	553	501	0,91
BPh 12	0,262	6107	461	384	0,83
TPh 3	0,219	5469	424	420	0,99
Ph 2	0,220	5473	412	419	1,02
Ph 4	0,223	5466	412	413	1,00
TPh 1	0,225	5355	392	401	1,02
TPh 4	0,257	5980	400	385	0,96
$20SiO_2 \cdot 80PbO$ (wt. %)	0,255	5030	290	327	1,13

$12Na_2O{\cdot}18RO{\cdot}70SiO_2$						
BeO		0,158	7890	600	777	1,30
CaO		0,218	7930	530	612	1,15
SrO		0,232	7650	530	555	1,05
BaO		0,252	7510	510	496	0,97
ZnO		0,222	6700	510	508	1,00
CdO		0,247	6810	510	461	0,90
PbO		0,217	5450	450	422	0,94
$Na_2O{\cdot}x\,RO{\cdot}5SiO_2$						
CaO	0,5	0,226	7350	492	548	1,11
	1,0	0,246	7300	521	496	0,95
	1,5	0,255	7700	558	501	0,90
	2,0	0,258	8000	583	513	0,88
	2,5	0,261	8050	600	509	0,85
	3,0	0,266	8800	633	542	0,86
ZnO	0,5	0,233	6900	480	498	1,04
	1,0	0,255	6950	508	452	0,89
	1,5	0,269	7200	537	437	0,81
	2,0	0,269	7250	542	440	0,81
	2,5	0,285	7400	546	413	0,76
	3,0	0,286	7900	566	438	0,77
SrO	0,5	0,238	7000	483	494	1,02
	1,0	0,259	7100	517	463	0,88
	1,5	0,263	7300	546	457	0,84
	2,0	0,274	7450	560	441	0,79

	2,5	0,282	7700	575	436	0,76
	3,0	0,280	8150	591	467	0,79
CdO	0,5	0,236	6505	475	463	0,97
	1,0	0,255	6495	500	423	0,85
	1,5	0,267	6500	517	398	0,77
	2,0	0,272	7050	525	421	0,80
	2,5	0,281	7050	533	402	0,75
	3,0	0,308	7100	542	347	0,64
BaO	0,5	0,239	6500	466	456	0,98
	1,0	0,258	6850	491	439	0,89
	1,5	0,270	6900	500	417	0,83
	2,0	0,281	6900	508	393	0,77
	2,5	0,285	6950	517	388	0,75
	3,0	0,286	6970	525	387	0,74
PbO	0,5	0,225	6030	433	451	1,04
	1,0	0,237	5650	442	400	0,90
	1,5	0,242	5700	417	395	0,95
	2,0	0,240	5600	417	391	0,94
	2,5	0,248	5300	392	357	0,91
	3,0	0,254	5020	350	328	0,94

Table 2.2

Mechanical properties of sulphate-phosphate glasses (Sanditov et al., 1993)

Glass	E / kg mm^{-2}	μ	f_g	A	H_V / kg mm^{-2}	P_m / kg mm^{-2}		$\frac{P_m}{H_v}$
						(3.19)	(3.16)	
$NaPO_3$	3610	0,294	0,016	1,08	175	195	194	1,11
$0,9NaPO_3 \cdot 0,1ZnSO_4$	4060	0,288	0,018	1,12	210	231	223	1,06
$0,8NaPO_3 \cdot 0,2ZnSO_4$	4220	0,284	0,019	1,13	225	248	237	1,05
$0,7NaPO_3 \cdot 0,3ZnSO_4$	4530	0,273	0,020	1,15	235	260	269	1,14
$0,6NaPO_3 \cdot 0,4ZnSO_4$	5210	0,259	0,020	1,15	260	286	332	1,28
$0,9NaPO_3 \cdot 0,1Li_2SO_4$	4140	0,300	0,014	1,05	200	206	212	1,06
$0,8NaPO_3 \cdot 0,2Li_2SO_4$	4210	0,303	0,013	1,04	200	205	212	1,06
$0,7NaPO_3 \cdot 0,3Li_2SO_4$	4230	0,304	0,014	1,05	215	212	212	0,99
$0,9NaPO_3 \cdot 0,1Na_2SO_4$	3730	0,299	0,016	1,08	195	207	192	0,98
$0,8NaPO_3 \cdot 0,2Na_2SO_4$	3550	0,292	0,016	1,08	190	191	190	1,00
$0,7NaPO_3 \cdot 0,3Na_2SO_4$	3540	0,288	0,015	1,07	180	172	194	1,08
$0,9NaPO_3 \cdot 0,1K_2SO_4$	3380	0,316	0,013	1,04	210	175	157	0,75
$0,8NaPO_3 \cdot 0,2K_2SO_4$	3350	0,316	0,014	1,05	205	185	156	0,76
$0,7NaPO_3 \cdot 0,3K_2SO_4$	3340	0,313	0,014	1,05	200	180	158	0,79
$0,4K_2SO_4 \cdot 0,6ZnSO_4$	2790	0,320	0,011	1,00	115	132	127	1,10

Table 2.3

Mechanical properties of $PbO–B_2O_3$ and $Bi_2O_3–B_2O_3$ glasses (Sanditov, Sangadiev, 1998)

Glass	μ	$E / 10^{-10}$ Pa	H_V / kg mm^{-2}	P_m / kg mm^{-2}	$\frac{P_m}{H_v}$
$PbO–B_2O_3$					
PbO, mol %					
0	0,262	1,728	194	111	0,57
25	0,268	5,593	385	348	0,90
30	0,276	5,934	389	354	0,91
35	0,275	6,230	412	373	0,91
40	0,276	6,409	414	383	0,93
42	0,275	6,347	412	380	0,92
44	0,276	6,470	392	385	0,98
45	0,276	6,141	395	366	0,93
46	0,278	6,235	385	369	0,96
48	0,276	6,132	384	366	0,95
50	0,278	6,033	382	357	0,93
55	0,283	5,418	331	312	0,94
60	0,285	4,954	302	281	0,93
65	0,285	4,431	272	252	0,93
70	0,287	4,101	247	231	0,94
$Bi_2O_3–B_2O_3$					
Bi_2O_3, mol %					

25,6	0,284	7,330	498	419	0,84
33,2	0,273	7,725	495	468	0,95
42,0	0,273	7,190	472	436	0,92
50,2	0,290	6,568	438	363	0,83
56,8	0,287	5,932	418	334	0,80

Figure Captions

Fig. 1. Schematics of the stress distribution along the symmetry axis z (broken line) for indentation of a solid with Poisson's coefficient $\mu = 0.3$ by spherical or Vickers indenter (ref. 1).

Fig. 2. Profiles of Vickers indentations at room temperature for aluminum at $P =$ 5 g (1), poly(methyl methacrylate) at $P = 10$ g (2) and silicate glass at $P = 20$ g (3) (ref. 17).

Fig. 3. Theoretical relationships between Vickers microhardness H_V and yield stress σ_y calculated by eq. (2.16) for $\mu = 0.3$ (curve 2), 0.2 (curve 3) and 0.1 (curve 4). The straight line 1 corresponds to $H_V/\sigma_y = 3$.

Fig. 4. Schematic representation of potential energy $U(r)$ and of interparticle interactions force $f(r)$ vs. interparticle distance.

Fig. 5. Schematics of temperature dependencies of thermodynamic properties for a substance in equilibrium crystal and molten states, and in non-equilibrium glassy states.

Fig. 6. Relationship between Vickers microhardness and glass transition temperature for inorganic glasses (ref. 1991).

Fig. 7. Relationship between Vickers microhardness and glass transition temperature for three series (circles, triangles and squares, respectively) of interpenetrating polymer networks (refs. 43 and 46).

Fig. 8. Schematics of temperature dependence of internal pressure of a substance in the equilibrium melt state, and in non-equilibrium glassy states.

Fig. 9. Relationship between yield stress and glass transition temperature for polymers (ref. 49).

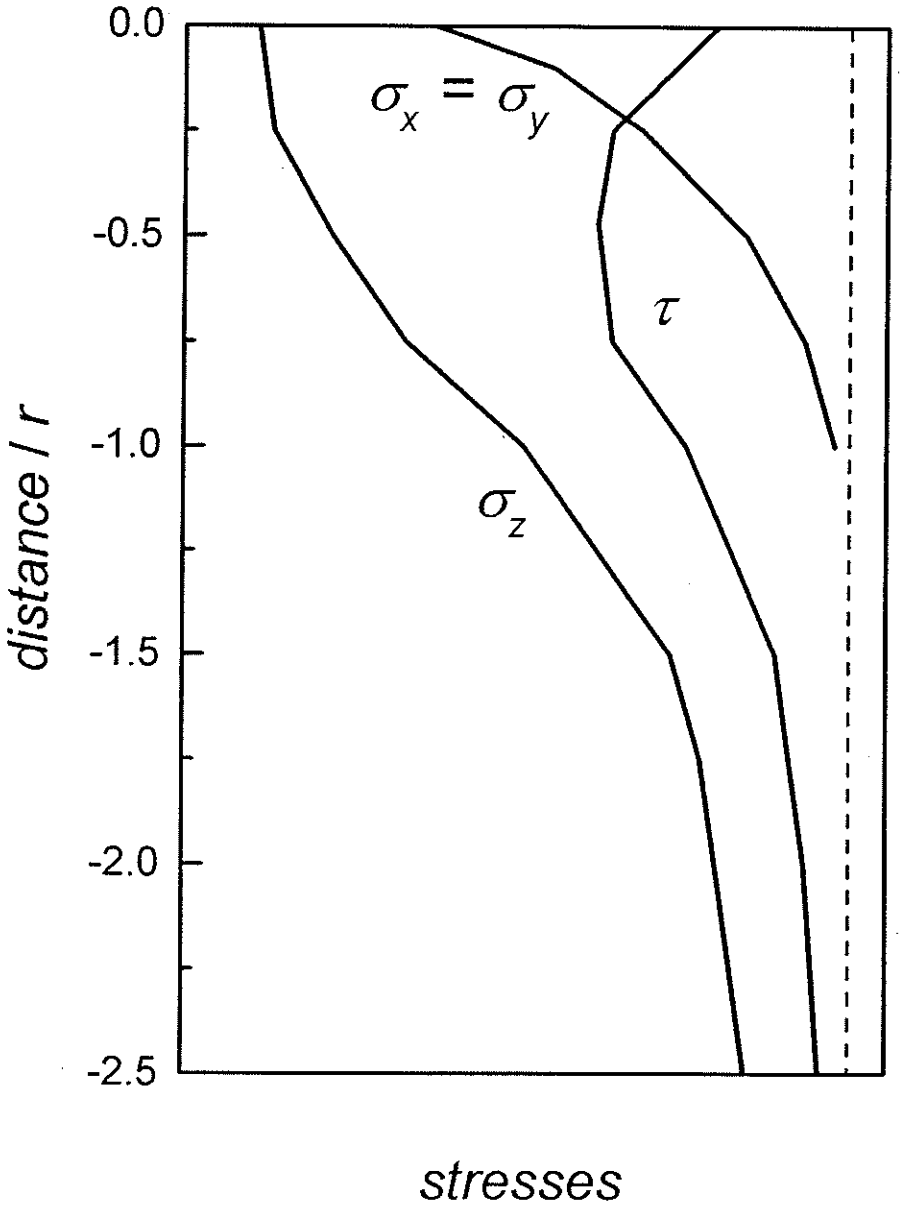
0.0
-0.5
-1.0
-1.5
-2.0
-2.5
distance / r
$\sigma_x = \sigma_y$
τ
σ_z
stresses

Fig. 1

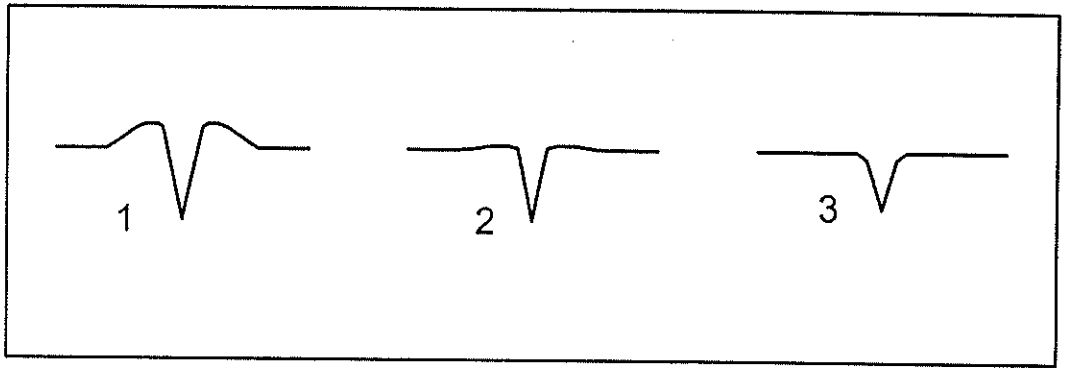

Fig. 2

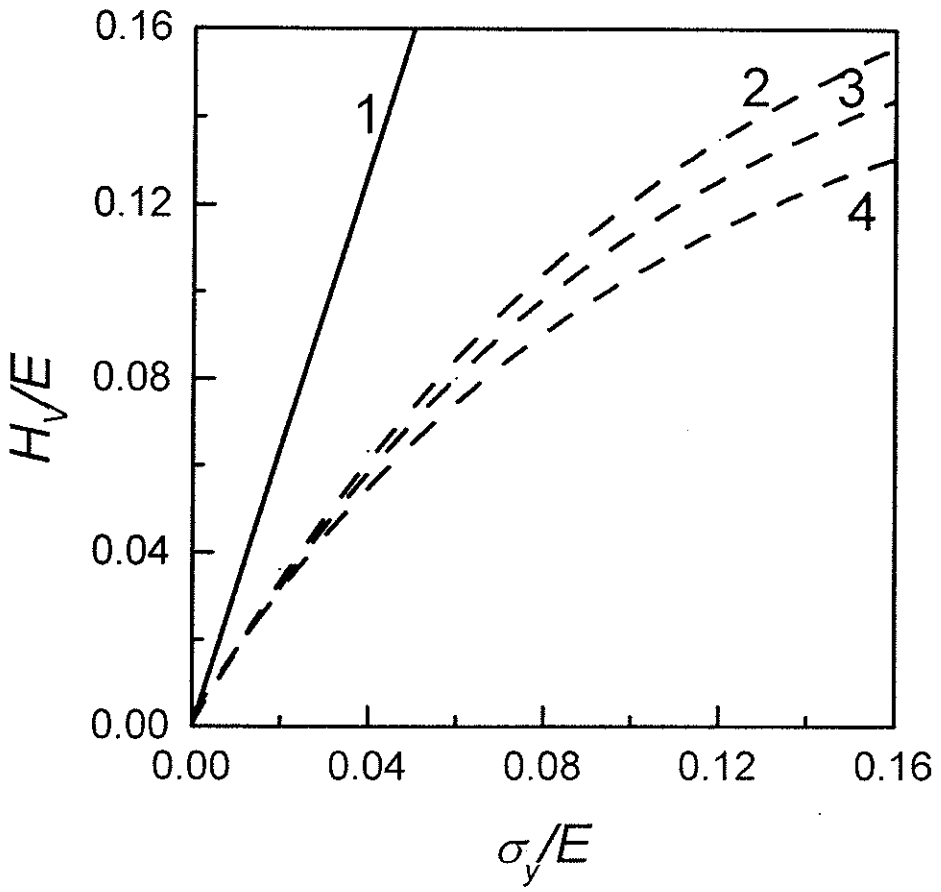

Fig. 3

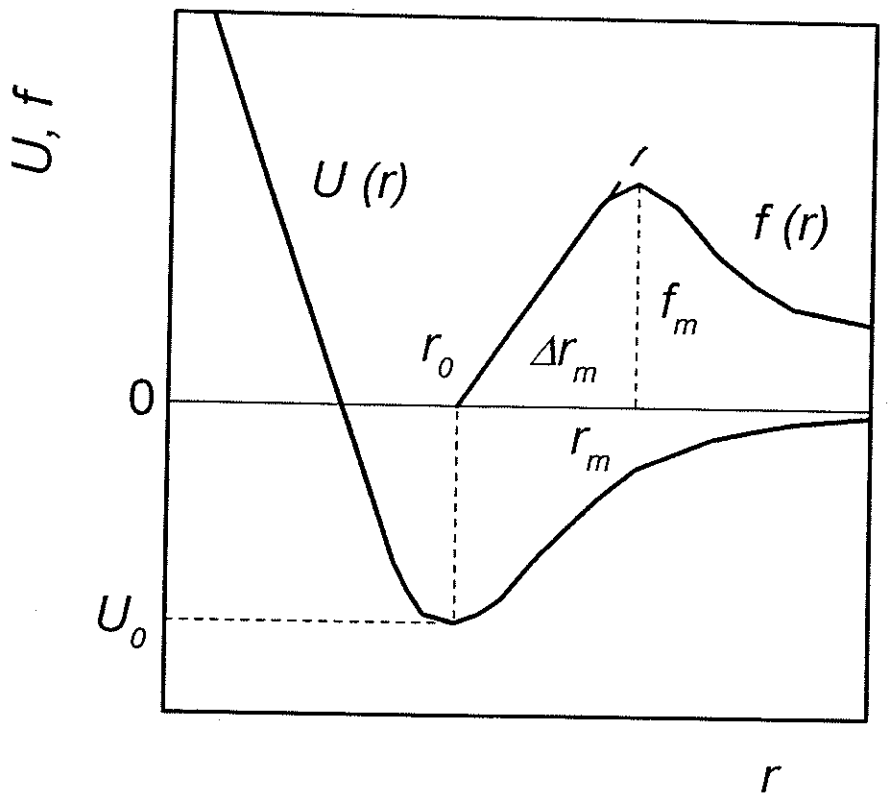

Fig. 4

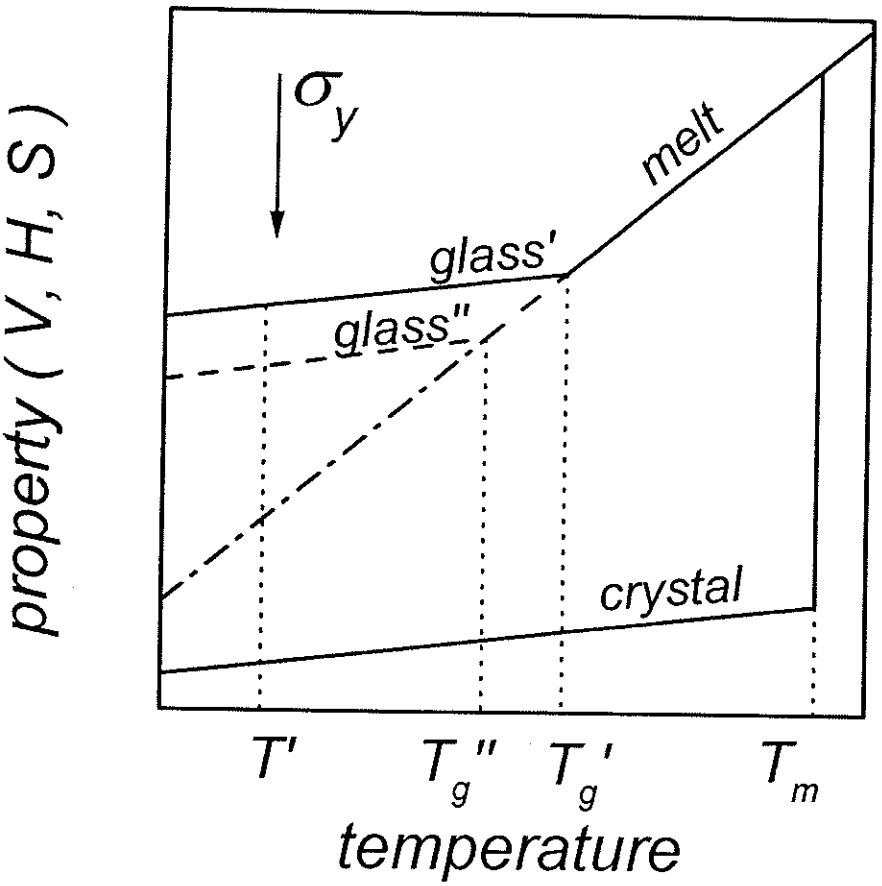
property (V, H, S)
σ_y
melt
glass'
glass"
crystal
T'
T_g"
T_g'
T_m
temperature

Fig. 5

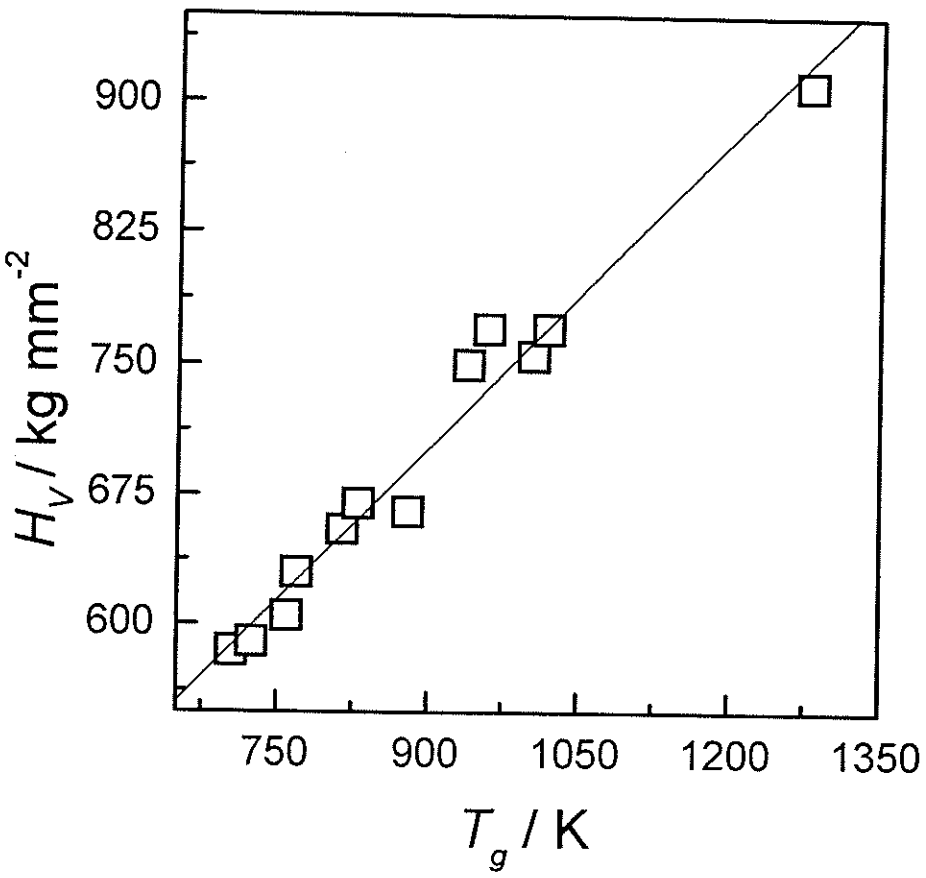

Fig. 6

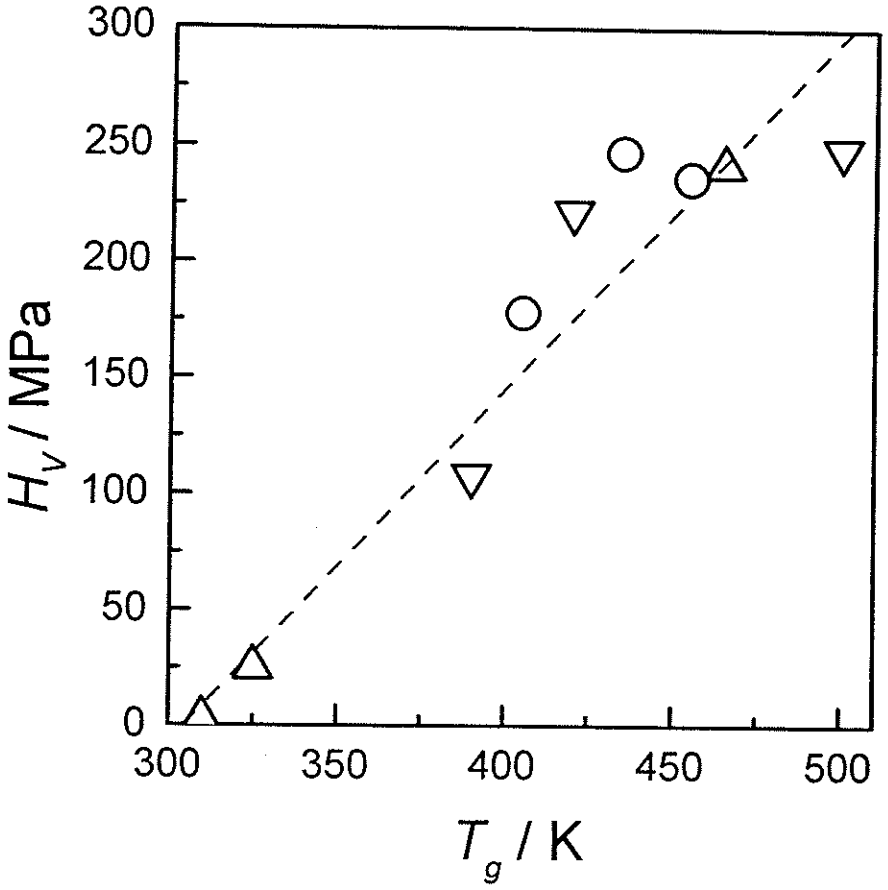

Fig. 7

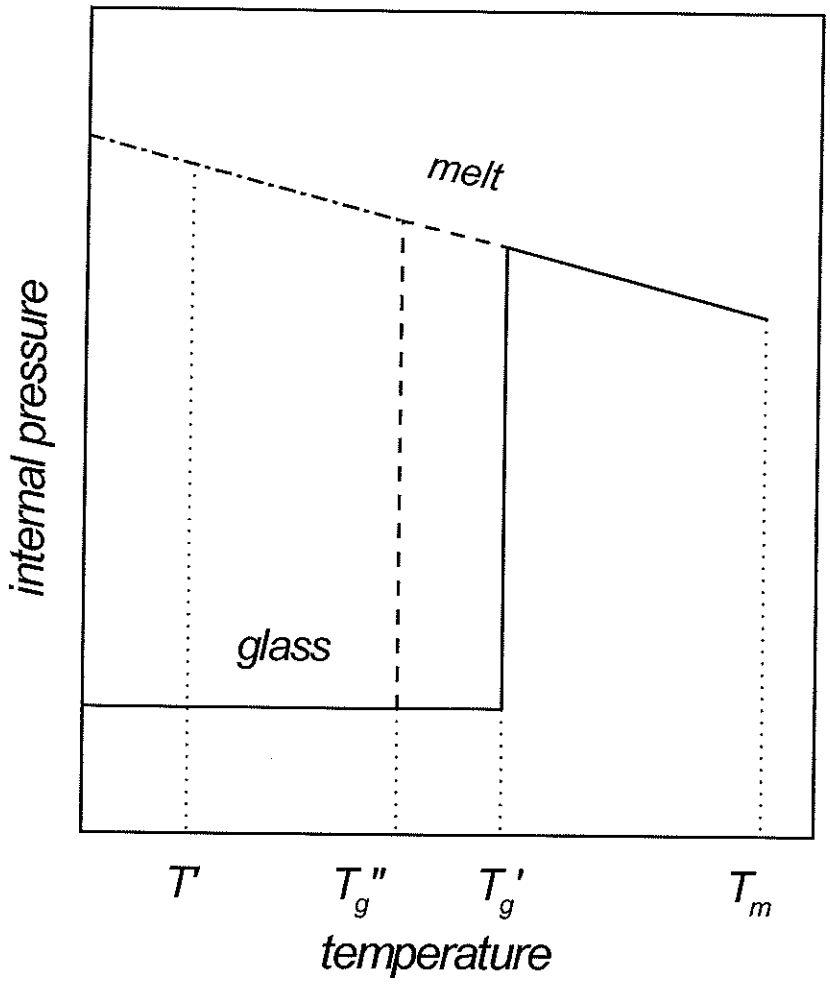

Fig. 8

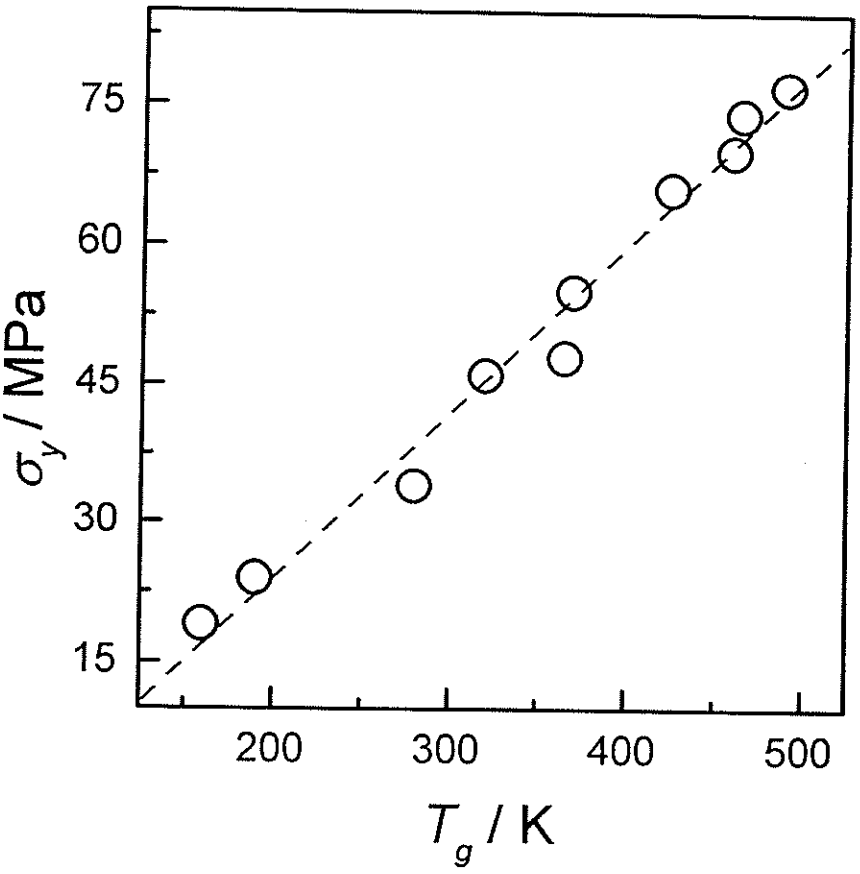

Fig. 9